Received: 28 February 2021 | Revised: 19 October 2021 | Accepted: 22 November 2021

DOI: 10.1111/joa.13603

Journal of Anatomy ANATOMICAL SOCIETY WILEY

ORIGINAL PAPER

The morphology of the subacromial and related shoulder bursae. An anatomical and histological study

Marion S. Kennedy | Helen D. Nicholson | Stephanie J. Woodley

Department of Anatomy, University of Otago, Dunedin, New Zealand

Correspondence
Marion S. Kennedy, Department of Anatomy, University of Otago, Dunedin, New Zealand.
Email: marionskennedy@gmail.com

Abstract

Shoulder bursae are essential for normal movement and are also implicated in the pathogenesis of shoulder pain and dysfunction. The subacromial bursa (SAB), within the subacromial space, is considered a primary source of shoulder pain. Several other bursae related to the subcoracoid space, including the coracobrachial (CBB), subcoracoid (SCB) and subtendinous bursa of subscapularis (SSB), are also clinically relevant. The detailed morphology and histological characteristics of these bursae are not well described. Sixteen embalmed cadaveric shoulders from eight individuals (five females, three males; mean age 78.6 ± 7.9 years) were investigated using macro-dissection and histological techniques to describe the locations, dimensions and attachments of the bursae, their relationship to surrounding structures and neurovascular supply. Bursal sections were stained with haematoxylin and eosin to examine the synovium and with antibodies against von Willebrand factor and neurofilament to identify blood vessels and neural structures respectively. Four separate bursae were related to the subacromial and subcoracoid spaces. The SAB was large, with a confluent subdeltoid portion in all except one specimen, which displayed a distinct subdeltoid bursa. The SAB roof attached to the lateral edge and deep surface of the acromion and coracoacromial ligament, and the subdeltoid fascia; its floor fused with the supraspinatus tendon and greater tubercle. The CBB (15/16 specimens) was deep to the conjoint tendon of coracobrachialis and short head of biceps brachii and the tip of the coracoid process, while the inconstant SCB (5/16 specimens) was deep to the coracoid process. Located deep to the subscapularis tendon, the SSB was a constant entity that commonly displayed a superior extension. Synovial tissue was predominantly areolar (SAB and SSB) or fibrous (CBB and SCB), with a higher proportion of areolar synovium in the bursal roofs compared to their floors. Blood vessels were consistently present in the subintima with a median density of 3% of the tissue surface area, being greatest in the SSB and SAB roofs (4.9% and 3.4% respectively) and least in the SAB floor (1.8%) and CBB roof and floor (both 1.6%). Nerve bundles and free nerve endings were identified in the subintima in approximately one-third of the samples, while encapsulated nerve endings were present in deeper tissue layers. The extensive expanse and attachments of the SAB support adoption of the term subacromial-subdeltoid bursa. Morphologically, the strong attachments of the bursal roofs and floors along with their free edges manifest as fixed and mobile portions, which enable movement in relation to surrounding structures. The presence of neurovascular structures demonstrates that

these bursae potentially contribute blood supply to surrounding structures and are involved in mechanoreception. The anatomical details presented in this study clarify the morphology of the shoulder bursae, including histological findings that offer further insight into their potential function.

KEYWORDS
anatomy, blood vessels, bursa, free nerve endings, shoulder, subacromial space, subcoracoid space, synovium

1 | INTRODUCTION

The shoulder is complex from functional and biomechanical perspectives, and contains a number of important structures, including bursae (Codman, 1934). While shoulder bursae are essential for normal movement, they are also implicated in the pathogenesis of shoulder pain and dysfunction (Moore, 2014; Rockwood et al., 2009) which affects a large proportion of adults, and increases with age (Djade et al., 2020; Hill et al., 2010; Luime et al., 2004; Taylor, 2005). The subacromial bursa (SAB), situated in the subacromial space, is the largest among the bursae associated with the shoulder (Codman, 1934), and functionally facilitates movement between the humeral head and coracoacromial arch. Clinically, the SAB is particularly relevant due to its potential involvement in subacromial pathology and pain (Cadogan et al., 2011; Codman, 1934; Lewis, 2009; Neer, 1983). Several other bursae, the coracobrachial (CBB), subcoracoid (SCB) and subtendinous bursa of subscapularis (SSB), which are related to the subcoracoid space, may also contribute to shoulder pathology (Colas et al., 2004; Drakes et al., 2015; Grainger et al., 2000; Pfuhl, 1934; Strizak et al., 1982).

Despite their clinical importance, many aspects of the morphology of the SAB and related shoulder bursae are not well established and the terminology is inconsistent (Kennedy et al., 2017). While it is agreed that the SAB is a constant structure, the presence of and communication with a subdeltoid bursa is less certain (Beals et al., 1998; Codman, 1934, Duranthon & Gagey, 2001; Federative International Programme for Anatomical Terminology, 2019; Seo et al., 2018; Strizak et al., 1982). Furthermore, there is debate around the constancy of the subcoracoid portion of the SAB or if there is communication between the SAB and a SCB or CBB (Codman, 1934; Gardner & Gray, 1953; Horwitz & Tocantins, 1938; Mitchell et al., 1988; Pfuhl, 1934). Although the general attachment sites of the SAB appear well defined, variability is evident concerning its precise attachment to surrounding structures such as the acromion, coracoacromial ligament, subdeltoid fascia, tendons of infraspinatus and subscapularis and the bicipital groove (Codman, 1934; Duranthon & Gagey, 2001; Mitchell et al., 1988; Pfuhl, 1934; Strizak et al., 1982; Yang et al., 2009). In relation to its medial-lateral extent, it is unclear whether the SAB reaches deep to the acromioclavicular joint and into the supraspinous fossa and inferior to the greater tubercle (Birnbaum & Lierse, 1992; Cooper et al., 1993; Nottage, 1993; Pfuhl, 1934). The morphology of the smaller shoulder bursae has been afforded less attention, but inconsistencies are evident. This is particularly true regarding the location, constancy, dimensions, attachment and communication of the bursae, including the relationship between the CBB and/or SCB with the superior extension of the SSB (Colas et al., 2004; Federative International Programme for Anatomical Terminology, 2019; Fick, 1904; Horwitz & Tocantins, 1938; Monro, 1799; Standring, 2016).

Little is known about the histological characteristics of the shoulder bursae, including synovial structure, and neurovascular supply (Kennedy et al., 2017). Descriptions of bursal synovium, in general, are scarce (Dunn et al., 2003; Hirschmann et al., 2007; Woodley et al., 2008), with this tissue depicted as being similar to that of synovial joints and tendon sheaths (Key, 1932) with a typical two-layer arrangement (intima or synovial lining and the underlying subintima; Firestein et al., 2017; Hirschmann et al., 2007; Mitchell et al., 1988; Sarkar & Uhthoff, 1983). The morphology of the SAB subintima has been documented in three studies, variably described as consisting of (1) loose connective tissue containing vascular channels, (2) dense irregular connective tissue interposed with loose areolar tissue or (3) mature adipose tissue (Mitchell et al., 1988; Sarkar & Uhthoff, 1983; Soifer et al., 1996).

An appreciation of the neurovascular supply of the subacromial and subcoracoid spaces, including the bursae, is essential due to bursal involvement in rotator cuff pathology (e.g. concomitant bursitis leading to nociception) and their relevance in surgical interventions (e.g. the SAB plays a key role in the rotator cuff healing process, a consideration for bursectomy) (Blaine et al., 2005; Brooks et al., 1992; Chillemi et al., 2016; Feldman, 2018; Lohr & Uhthoff, 1990; Nam et al., 2018; Rathbun & Macnab, 1970; Uhthoff & Sarkar, 1991; Yepes et al., 2007). Both joint and bursal synovium are well vascularised (Dunn et al., 2003; Hirschmann et al., 2007; Key, 1932; Sarkar & Uhthoff, 1983; Wilkinson & Edwards, 1989), but the few available descriptions of the blood supply of the shoulder bursae have solely considered the SAB (Determe et al., 1996; Yepes et al., 2007). Neural structures, including nerve fibres, free nerve endings and various other mechanoreceptors have been identified in the subintima of the SAB, suggesting both nociceptive and proprioceptive functions (Ide et al., 1996; Soifer et al., 1996; Tomita et al., 1997; Vangsness et al., 1995). However, only one of these studies used specific antibodies to detect nerve tissue in the SAB (Soifer et al., 1996) and data on the neurovascular supply of the CBB, SCB and SSB have not been published.

In order to address some of the gaps in the literature, the aims of this study were to: (1) investigate the gross morphology of the shoulder bursae, particularly to better document precise dimensions and attachments, communication and relationship with surrounding bursae; and (2) examine the microarchitecture of the shoulder bursae, including the types of synovial tissue, the presence and density of blood vessels and the types and location of nerve endings.

2 | METHODS

2.1 | Specimens

Sixteen paired shoulders from eight embalmed human cadavers (five females, three males) with a mean age of 78.6 ± 7.9 years (range 67–91 years) were dissected. All cadavers were from a New Zealand European population bequeathed to the Department of Anatomy, University of Otago, in accordance with the New Zealand Human Tissue Act (2008). Departmental ethical approval was received for this study. Causes of death/comorbidities included cardiovascular disease ($n = 6$), oesophageal carcinoma ($n = 1$) and Alzheimer's disease ($n = 1$). The average time between death and dissection was 20.0 ± 8.7 months. Prior to dissection, radiographs were taken of each specimen. No evidence of glenohumeral osteoarthritis was found; the subacromial space was mildly ($n = 1$) or moderately ($n = 3$) narrowed, and otherwise unremarkable. Mild ($n = 6$) and moderate ($n = 1$) bony irregularity was seen at the rotator cuff insertion. Osteoarthritic changes in the acromioclavicular joint were present in five shoulders.

All SAB were injected with latex under real-time ultrasound guidance by an experienced sonographer using an anterolateral approach (Mathews & Glousman, 2005; Molini et al., 2012). Latex (range 3–8 ml) was injected (using an 18 gauge needle) until pressure build-up within the syringe prevented any more being added, and latex distribution was encouraged by gently massaging and passively moving the shoulder (Beals et al., 1998). The specimens were then placed in a neutral shoulder position until the latex had solidified. During dissection, other bursae identified were also injected with latex (1.0 ± 0.7 ml). Following dissection, the bursal surface of the rotator cuff was examined macroscopically for the presence of full-thickness tears, graded based on their anterior-posterior extent (Hijioka et al., 1993). Bursae were excluded from the analysis if bursal boundaries were not verifiable due to rotator cuff pathology or if histological analysis did not confirm bursal synovium.

2.2 | Dissection

Specimens were dissected using a 1.5 times magnification lens (laboclip, Eschenbach). Skin, superficial fascia and superficial musculature were removed. The conjoint tendon and the pectoralis minor tendon were transected ~5 cm below their proximal attachment. The deltoid was detached from its insertions on the humerus, clavicle and spine of the scapula and reflected proximally towards the acromion, and the course of the anterior branch of the axillary nerve was marked on the humerus (Cooper et al., 1993).

The subdeltoid fascia was reflected towards the acromion to expose the SAB roof and the attachment between the two structures was marked (Cooper et al., 1993). The spine of the scapula and the clavicle were transected and the coracoacromial ligament resected at its coracoid insertion. Then, the SAB roof was opened and the latex within the cavity was removed. Next, the acromion was reflected to fully expose the extent of the SAB (Birnbaum & Lierse, 1992; Hijioka et al., 1993; Pfuhl, 1934).

The bursae related to the conjoint tendon and/or coracoid process were exposed by reflecting the conjoint tendon superiorly and then transecting the coracoid process close to its root. Bursae located deep to the conjoint tendon and the tip of the coracoid process were defined as CBB, and those confined deep to the coracoid process were classified as SCB (Kennedy et al., 2017). To expose the SSB, subscapularis was released from its medial attachment in the subscapular fossa and reflected laterally towards the lesser tubercle (Colas et al., 2004).

The location of each bursa and attachments of their roofs and floors and their relationships to each other and surrounding structures were described and marked with pins or water-insoluble ink.

2.3 | Bursal and skeletal landmark measurements

Figure 1 details the measurements taken during dissection, first with the acromion *in situ* and the SAB intact (Beals et al., 1998; Fremerey et al., 2000). Then, with the acromion removed, the SAB roof attachment (anterior-posterior and medial-lateral) to the deep surface of the acromion and coracoacromial ligament was measured (Pfuhl, 1934). The terms medial and lateral were used to describe the superomedial and inferolateral extents of the SAB floor respectively. The dimensions of the exposed bursal floors were measured at their widest points (Birnbaum & Lierse, 1992), and the extent and attachment of a superior extension of the SSB were documented. All distances were measured in cm (±0.1 cm) using a flexible standard tape measure (0–150 cm) with the humerus in a neutral position in relation to the scapula.

2.4 | Histology

Bursal samples ($n = 182$; ≤1 cm^2 in size) were harvested from the roofs and the floors of the various bursae from areas with macroscopically intact underlying rotator cuff tendons. Samples were placed into 10% neutral buffered formalin and embedded in paraffin. Sections were cut at 4 μm using a Leica–RM microtome (Leica Microsystems) and placed onto glass slides.

To enable examination of the synovium all sections were stained with haematoxylin and eosin (H&E). For immunohistochemistry, 47 samples from four females (two right, two left) and four male

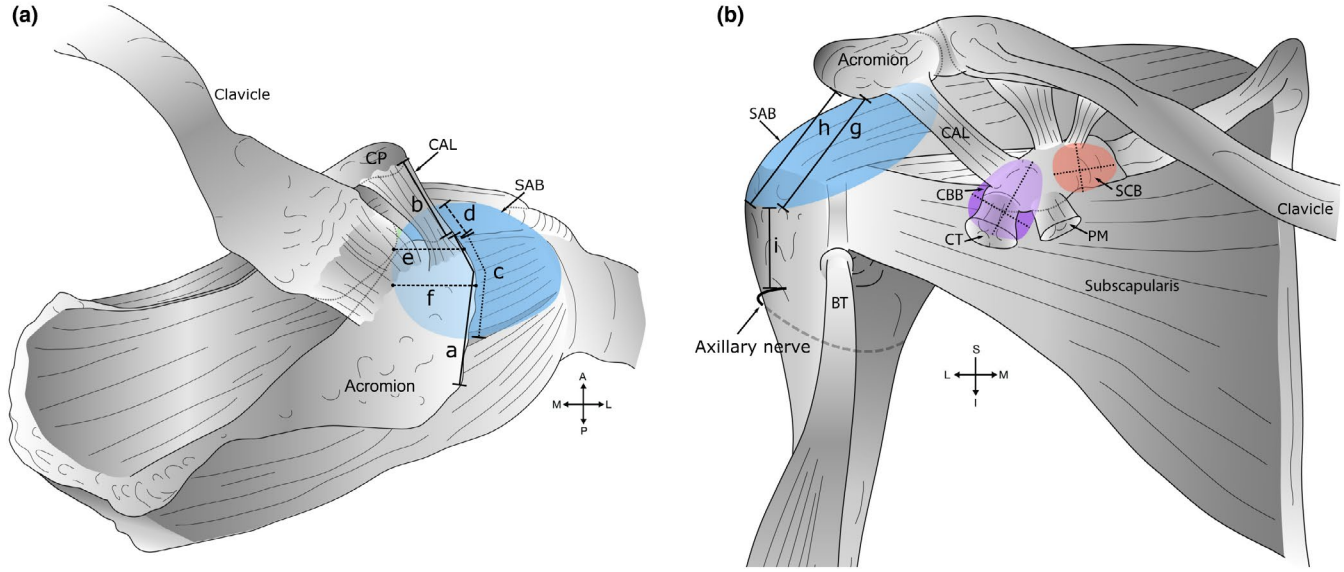

FIGURE 1 Measurements of bursae and skeletal landmarks. A schematic diagram outlining measurements of bursae obtained during dissection. (a) Superior view. Key: (a) Acromial length. The midpoint of the acromion was defined as half of the acromial length; (b) coracoacromial ligament (CAL) length; (c) anterior-posterior extent of the subacromial bursa (SAB) along the acromion and (d) coracoacromial ligament; (e) medial extent of the SAB from the anterolateral corner of the acromion; (f) medial extent of the SAB from the midpoint of the acromion, and in relation to the acromioclavicular joint—medial or lateral to the plane of the joint (descriptive only). Measurements 'e' and 'f' were aligned along the fibres of supraspinatus. (b) Anterior view. Key: Inferior extent of the SAB from the (g) anterolateral corner and (h) midpoint of the acromion; (i) distance from the inferior extent of the SAB to the axillary nerve (anterior branch). Measurements 'h–i' were aligned with the shaft of the humerus. Medial-lateral and superior-inferior dimension of the coracobrachial (CBB) (shaded purple) and subcoracoid (SCB) bursa (shaded orange), deep to the coracoid process (CP) and conjoint tendon (CT) of coracobrachialis and the short head of biceps brachii. Abbreviations: A, anterior; BT, biceps tendon (long head); I, inferior; L, lateral; M, medial; P, posterior; PM, pectoralis minor; S, superior

(two right, two left) specimens (six paired; two unpaired), were chosen from the existing tissue blocks, representing all investigated bursae. Two sections were obtained for H&E and if a block was used for immunohistochemistry, a further two sections were taken. For immunohistochemical staining, antibodies against von Willebrand factor and neurofilament were used to selectively detect blood vessels specifically and myelinated and non-myelinated nerve fibres respectively. Von Willebrand factor is a glycoprotein in the cytoplasm of human endothelial cells from blood vessels (Pan et al., 2016; Pusztaszeri et al., 2006), and neurofilament protein occurs in the cytoplasm of neurons providing structural support (Ross, 2006). Endogenous peroxidase activity was blocked by placing the slides in 3% methanolic hydrogen peroxide for 10 min. A heat-mediated (60°C) antigen retrieval was performed for 16 h using either a pH 9.0 Tris ethylenediaminetetraacetic acid (von Willebrand) or pH 6.0 citrate (neurofilament) buffer. Then, sections were protein blocked using 10% bovine serum albumin (BSA; Gibco, Thermo Fisher, NZ) for 30 min. The primary (Rabbit anti-von Willebrand factor polyclonal raised in rabbit, anti-human, 1:400 dilution, Dako Agilent, Denmark; Mouse anti-neurofilament monoclonal, 1:2500 dilution, Covance, USA) and secondary (EnVision + Dual link system-horse radish peroxidase-labelled polymer, Dako Agilent Denmark) antibodies were applied. Following this, 3,3' diaminobenzidine (DAB) chromogen solution (1 drop DAB in 1 ml DAB buffer; Cell Marque, Merck, Germany) was applied to each slide for 5 min. On slides receiving neurofilament antibody, DAB enhancer (Bond, Leica Biosystems) was applied for 5 min following the application of the chromogen solution. Positive and negative (omitting the primary antibody) control sections from embalmed human sciatic nerve with intrinsic blood vessels were included in each immunohistochemical run. All slides were counterstained with Mayer's haematoxylin.

2.5 | Histology analysis

From the H&E stained sections, the presence and type of synovium were observed and categorised as described by Key (1932) as areolar, fibrous or adipose by MSK using an Olympus AX 70 light microscope (Olympus Corporation). Photomicrographs were taken using a MicroPublisher RT digital camera (QImaging, Surrey). If uncertainty existed with classification, photomicrographs were analysed independently by SJW to reach a consensus.

For quantitative analysis of blood vessels and nerves, immunohistochemistry slides were digitised at 400× magnification and calibrated using the Aperio CS ScanScope scanner and ImageScope software respectively (Aperio Technologies, Leica Biosystems) and analysed using ImageJ software (National Institute of Health, University of Wisconsin). Areas containing intact intima and underlying subintima were traced using the polygon selection tool to provide a measurement of surface area (mm^2). Artefactual spaces,

TABLE 1 Types, number and dimensions of bursae

Type of bursa (number of specimens included)	Bursae number (%)	Dimensions, mean ± SD (range) in cm, measurement direction	
Subacromial (14)	14 (100)	5.6 ± 1.6 (2.1–8.0), anterior-posterior	6.0 ± 1.6 (3.7–9.2), medial-lateral
Subdeltoid (14)	1 (7)	3.8, anterior-posterior	2.5, medial-lateral
Coracobrachial (16)[a]	15 (93.8)[b]	2.3 ± 1.0 (0.9–3.7), medial-lateral	2.6 ± 0.9 (1.2–4.8), superior-inferior
Subcoracoid (16)[a]	5 (31.2)[b]	1.5 ± 0.5 (0.9–2.2), medial-lateral	1.6 ± 0.5 (1.0–2.3), superior-inferior
Subtendinous bursa of subscapularis (16)	16 (100)	2.8 ± 1.0 (0.8–4.8)[c], medial-lateral	2.6 ± 1.1 (1.3–4.5)[c], superior-inferior

[a]Distribution of CBB and SCB in specimens: single CBB: $n = 11$; one CBB and one SCB: $n = 4$; one single SCB: $n = 1$.

[b]Bursa excluded because synovial lining was not confirmed histologically: $n = 3$ (CBB: $n = 1$, in one specimen with two CBB), and $n = 2$ SCB ($n = 1$ in one specimen with two SCB; $n = 1$ single SCB).

[c]Measurement data available from $n = 15$ specimens.

defined as spaces within the region of interest (ROI) that did not contain tissue (e.g. where tissue layers had separated), were traced and measured in the same manner. The sum of the area of artefactual spaces was deducted from the area of the original tissue outline to obtain the surface area of the ROI (mm^2). On each section, the outline of each blood vessel was traced, and individual surface areas (mm^2) were summed. Neural structures were classified as nerve bundles and free or encapsulated nerve endings (Rein et al., 2013; Ross, 2006; Stecco et al., 2018; Yeo et al., 2016) and their location was documented.

For both H&E and immunohistochemistry, sections were excluded from analysis if (1) synovial lining was absent, (2) analysis was precluded by tissue damage or background staining or (3) immunoreactivity was absent.

2.6 | Statistical analysis

Excel for Mac (Version 15.25, Microsoft Corporation) and IBM SPSS statistics programme for Windows (Version 25.0, IBM Corporation Armonk) were used for descriptive statistics and additional calculations respectively. The extent of the SAB along the acromion and coracoacromial ligament was expressed as a percentage of the anterior-posterior length of the acromion and coracoacromial ligament respectively (Beals et al., 1998; Birnbaum & Lierse, 1992).

Histological results from the CBB and SCB were combined. Frequencies of the three categories of synovium (areolar, fibrous, adipose) were expressed as percentages for the SAB, CBB/SCB and SSB, their roofs and floors, as well as the proximal, middle and distal areas for the SAB roof and floor. For statistical comparison, the three categories of synovium were collapsed into two: Category 1: areolar, and category 2: non-areolar (including fibrous and adipose; Field, 2013). The same was repeated for fibrous and adipose synovium respectively. The proximal, middle and distal areas of the SAB roof and floor were combined into two categories: Category 1: proximal and middle area, and category 2: distal area. Differences were examined using Pearson's chi-square test or Fisher's exact test ($\alpha = 0.05$) with follow-up adjustment of alpha values ($\alpha = 0.017$) using the Bonferroni correction for multiple tests (Field, 2013; Hall & Richardson, 2016; Kim, 2017).

Blood vessel density was calculated as a percentage of the area of the ROI that was occupied by blood vessels for each section (Perumal et al., 2019). The median and interquartile range (IQR) of blood vessel density were calculated for all samples combined, and for specific areas of each bursa. Blood vessel density between the roofs of the SAB, CBB and SSB was compared with an independent samples Kruskal–Wallis test ($\alpha = 0.05$), with follow-up adjustment as described above. An independent-samples Mann–Whitney U test (2 samples, $\alpha = 0.05$) was used to analyse differences between the (1) floor of the SAB and CBB, (2) SAB roof and floor, (3) CBB roof and floor and (4) proximal and distal areas of the SAB roof.

3 | RESULTS

Of the 16 shoulder specimens, two were excluded from analyses relating to the SAB due to massive rotator cuff tears, which meant the bursal boundaries were lost or only partially verifiable. Four other specimens presented with full thickness rotator cuff tears, ranging in size from small ($n = 1$) to moderate-large ($n = 3$), with no tendon pathology noted in 10 specimens. Three bursae (one CBB, two SCB) identified during dissection were excluded, because the presence of synovium was not confirmed histologically, secondary to tissue damage.

Table 1 presents the type, number and dimensions of bursae that were identified in the cadaveric specimens.

3.1 | Subacromial bursa

The SAB was consistently present as a large, round separate structure located deep to the acromion, the coracoacromial ligament and the proximal deltoid muscle and subdeltoid fascia. One specimen displayed a separate SAB and SDB. In this case, the SAB was confined deep to the acromion, triangular-shaped and relatively small. The SDB was posterolateral to the SAB, extending about 3 mm over the teres minor tendon; its roof weakly attached to the subdeltoid fascia and did not reach the acromion.

In 15 specimens, the SAB roof consistently displayed strong fascial connections to the acromion, coracoacromial ligament and subdeltoid fascia (Table 2). It attached to the anterolateral acromial edge and lateral aspect of the coracoacromial ligament (Figure 2a–c) and was firmly attached to the deep surface of the acromion, commonly in an oval shape. Posterior to the midpoint of the acromion, the SAB roof continued for up to 1.8 cm, folding in on itself. It usually encompassed the deep surface of the coracoacromial ligament, variably including between half to nearly the whole length and whole width of the ligament (Table 2). Medially, the SAB roof reached the deep surface of the acromioclavicular joint capsule where it was attached to overlying subacromial fat and to the deep aspect of the capsule. In 64% of cases, the SAB continued medial to the acromioclavicular joint plane, predominantly involving the anterior half of the joint. In all specimens, the roof was strongly connected to the overlying subdeltoid fascia. In some (5/16), deltoid muscle fibres fused with the underlying subdeltoid fascia over its attachment area with the roof. The floor of the SAB was intimately associated with three of the rotator cuff tendons (supraspinatus, infraspinatus, subscapularis), the bicipital groove and the greater and lesser tubercles (Figure 2d–f). Usually, the SAB floor covered and was firmly attached to the supraspinatus tendon and the greater tubercle (superior facet). The extent over the supraspinatus muscle and inferior to the greater tubercle as well as the relationship to the remaining underlying structures was more variable.

TABLE 2 Morphometric data relating to the subacromial bursa

Bursa or landmark of interest (data from 14 specimens, unless stated)	Measurements mean ± SD (range) in cm (or % if stated)
Acromion length	5.1 ± 0.7 (4.3–6.6)
CAL length	3.9 ± 0.6 (2.7–5.2)
SAB roof extent (acromion *in situ*)	
Along acromion, anterior-posterior	2.9 ± 1.0 (1.6–4.9)
As percentage of acromion length (%)	58.2 ± 21.1 (30.8–100)
Along CAL, anterior-posterior	3.4 ± 0.7 (1.0–4.1)
As percentage of CAL length (%)	72.0 ± 15.4 (25.0–89.1)
Along lateral edge of acromion and CAL, anterior-posterior	5.5 ± 1.2 (3.2–7.2)
SAB roof extent (acromion reflected)	
On deep surface of acromion	
Anterior-posterior	2.4 ± 0.6 (1.1–2.2)
Medial-lateral	1.7 ± 0.7 (0.4–2.9)
On deep surface of CAL	
Anterior-posterior ($n = 8$)	2.6 ± 0.4 (1.9–3.2)
Medial-lateral (whole width, $n = 7$)	2.2 ± 0.6 (1.4–3.0)
On deep surface of acromion and CAL	
Anterior-posterior ($n = 5$)	4.4 ± 0.9 (3.2–5.5)
Lateral extent of SAB floor (acromion *in situ*)	
From anterolateral tip of acromion	4.1 ± 1.1 (2.5–6.0)
From midpoint of acromion ($n = 12$)	3.4 ± 0.7 (2.4–5.2)
Distance between most lateral extent of SAB and axillary nerve ($n = 11$)	3.4 ± 1.6 (1.2–6.0)
Medial extent of SAB	
From anterolateral tip of acromion ($n = 13$)	2.4 ± 1.1 (1.1–4.3)
From midpoint of acromion ($n = 10$)[a]	2.1 ± 1.0 (0.8–3.6)

Abbreviations: CAL, coracoacromial ligament; SAB, subacromial bursa.
[a]Measurements presented include cases in which the most medial extent of the SAB was oriented in a straight line in relation to the fibres of the supraspinatus muscle.

3.2 | Coracobrachial and subcoracoid bursae

Across the 16 specimens, 20 bursae ($n = 15$ CBB, $n = 5$ SCB) were identified deep to the conjoint tendon and/or the coracoid process. These bursae were located in the same tissue plane as the SAB. Their dimensions and relationships with surrounding structures are detailed in Tables 1 and 3 and shown in Figure 3. Coracobrachial bursae were present in all but one specimen and were usually circular, oval or kidney-shaped. They were consistently localised deep to the conjoint tendon, extended for a variable distance deep to the tip of the coracoid process and overlay the subscapularis tendon. Subcoracoid bursae were mainly confined deep to the coracoid process, closely related to its root and vertical part, overlying the superior edge of the subscapularis tendon. In specimens which displayed both a CBB and a SCB ($n = 4$), the SCB was usually the smaller, more rounded structure.

3.3 | Subtendinous bursa of subscapularis and superior extension

The SSB displayed a constant main portion and a variable superior extension. The main portion was oval and of variable size (Table 1), located deep to subscapularis which separated it from the CBB, SCB and SAB (Table 3). The SSB roof was attached to the deep surface of the upper portion of the subscapularis tendon and adjoining muscle fibres. The floor of the SSB overlay, and was attached to, the root of the coracoid process, neck of the scapula and the anterior aspect of the glenohumeral joint capsule (Figure 4a).

The majority of SSB displayed a superior extension. This portion extended superior to the subscapularis tendon and passed deep to the coracoid process, where it attached to the periosteum of the root of the coracoid process and surrounding connective and fatty tissue. In nearly two-thirds of specimens, the superior extension projected over and along the upper edge of the subscapularis tendon, and overhung it anteriorly (Figure 4b; Table 3).

3.4 | Relationships between the bursae

No communication was confirmed between any of the bursae, with the exception of one CBB that communicated with a SAB via a small hole through a shared wall. Up to three bursae (CBB, SCB, superior extension of SSB) were present in close proximity in the relatively

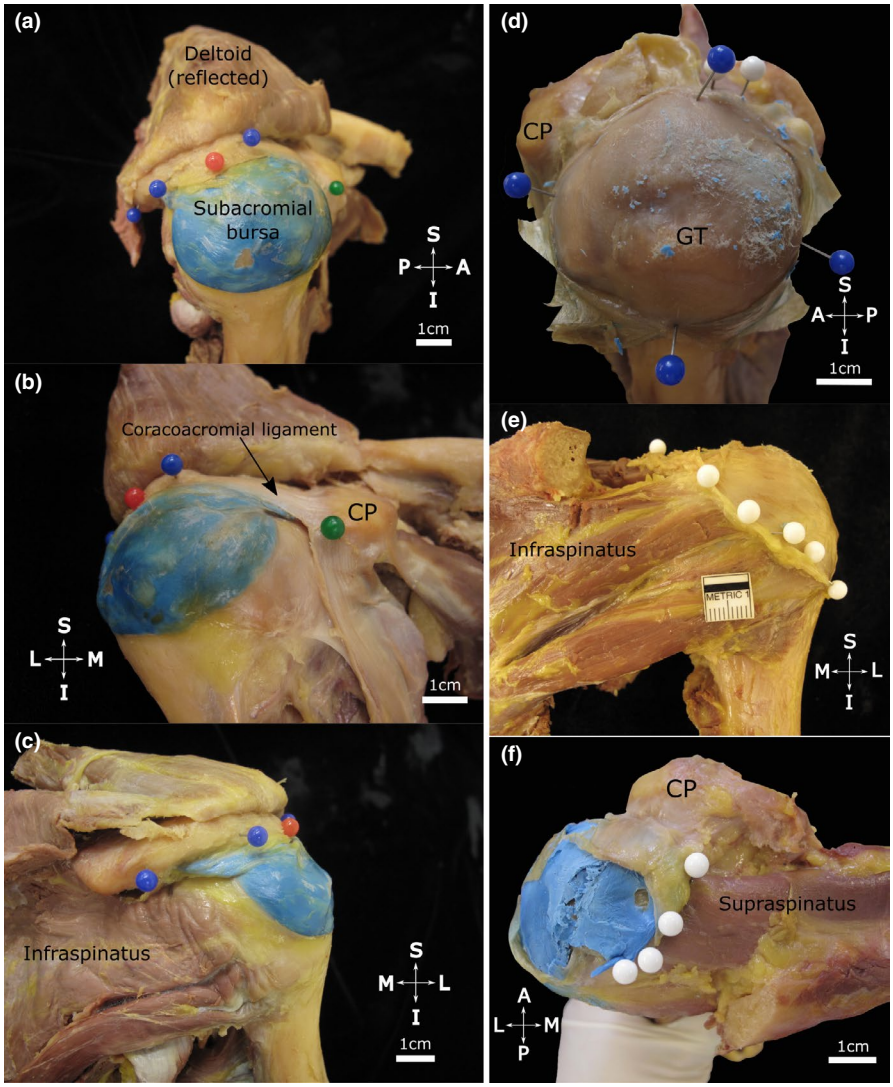

FIGURE 2 Extent of the subacromial bursa with the coracoacromial arch *in situ* (a–c) and after resection of the acromion (d–f). The subacromial bursa (injected with blue latex) is situated over the proximal humerus. Note (a, lateral view) its extent along the lateral edge of the acromion (blue pins) including the (b, anteromedial view) coracoacromial ligament anteriorly (black arrow) towards the coracoid process (CP, green pin). Posteriorly (c, posterior view) it extends towards the posterior aspect of the acromion. The red pin marks the midpoint of the acromion. (d–f) The acromion has been resected and the roof of the subacromial bursa has been opened and reflected to expose its floor. Note its (d, superolateral view) medial-lateral and anterior-posterior dimensions (blue pins), (e, posterior view) posterior extent (white pins) over the infraspinatus tendon and (f, superior view) medial extent (white pins, blue latex from injection *in situ*) overlying the supraspinatus tendon/muscle in the supraspinous fossa. Abbreviations: A, anterior; GT, greater tubercle; I, inferior; L, lateral; M, medial; P, posterior; S, superior. Scale bar marked in cm

small area deep to the (proximal) coracoid process and acromial part of the coracoacromial ligament, sometimes bordering on each other and/or overlapping (Figure 3). As an associated finding, the SSB communicated in the majority of cases with the glenohumeral joint via an aperture in the anterior-superior aspect of the capsule.

3.5 | Bursal synovium

From the 182 samples, 139 sections were suitable for inclusion in the analysis (43 were excluded due to tissue damage). Three types of bursal synovium were identified in the bursae (Figure 5). All bursal samples combined showed predominantly areolar synovium (55%), followed by fibrous (33%), with adipose being the least common (12%). The distribution of the type of synovium varied between the three bursal locations (Figure 5), bursal roofs and floors and the proximal and distal SAB roof and floor (Table S1). Areolar synovium was predominant in all of the roofs (47%–70%) and the SAB floor (48%), while the floors of the CBB/SCB and SSB were predominantly fibrous (both 67%). In the SAB roof and floor, areolar synovium was most prevalent proximally deep to the coracoacromial arch (roof 81%, floor 55%) and least common distally in the region of the greater tubercle (roof 50%, floor 42%). Fibrous synovium followed an opposite pattern, being least common proximally (roof 5%, floor 27%) and most

TABLE 3 Location and relationships between the bursae related to the subcoracoid spaces

	CBB	SCB	SSB	Superior extension of the SSB
General location/ relationships with landmarks	- Deep to conjoint tendon (constant) and tip of CP (13/15 specimens) - Deep to conjoint tendon (2 specimens) - Protrudes laterally (common) and medially (some specimens) to conjoint tendon - Extent superior to tip of CP: 1.2 ± 0.4 cm, range: 0.8–2.0 cm; 8/13 specimens - Extent inferior to tip of CP: 2.6 ± 0.7 cm, range: 1.1–3.7 cm; 8/15 specimens	- Usually deep to CP (root and vertical part) and acromial part of CAL (variable) - Floor extends inferior to tip of CP (2 specimens)	- Deep to upper portion of the subscapularis tendon (constant)	- Deep to CP, root and vertical part (13/16 specimens) - Extends along and anterior to the upper edge of subscapularis tendon (10/16 specimens)
Connections	**Roof:** Underlies and connects to conjoint tendon[a] (constant) and tip of CP (variable) **Floor:** Overlies and connects to subscapularis tendon **Lesser tubercle:** - Reaches up to medial edge of lesser tubercle (usual) - Covers lesser tubercle, medial half ($n = 1$), fully ($n = 1$)	**Roof:** Connects to deep surface (periosteum and connective tissue) of CP (root and vertical part) (constant) and to deep surface of acromial part of CAL (variable). **Floor:** Overlies and connects to superior aspect of subscapularis tendon and superior extension of SSB (if present)	**Roof:** Attaches to upper portion of deep surface of the subscapularis tendon and adjoining muscle fibres **Floor:** Connects to root of CP, neck of scapula, anterior aspect of glenohumeral joint capsule	- Connects to periosteum of CP (root) and surrounding connective and fatty tissue - Connects to upper edge of subscapularis tendon for 4.3 ± 1.2 cm - Overhangs the upper edge of the subscapularis anteriorly (mean 0.5 cm; range 0.3–0.7 cm).
Communication/ relationship with other bursae	- Communication with SAB via small hole through shared wall ($n = 1$) - Contiguous wall with SAB ($n = 4$) - Usually separate from SAB (0.7 ± 0.4 cm, range: 0.2–1.3 cm, data from $n = 6$ specimens) - Contiguous wall with SCB ($n = 1$) - No communication with SCB, SSB	No communication with SAB, CBB, SSB	- No communication with SAB, CBB, SCB - Communication with glenohumeral joint in 94% (15/16 specimens) between the superior and middle glenohumeral ligaments ($n = 14$), superior and inferior glenohumeral ligament ($n = 1$).	- No communication with SAB, CBB, SCB - Close proximity to CBB ($n = 7$) or SCB ($n = 4$) - Borders on or shares a wall with CBB or SCB (5/11 specimens) - Positioned deep to a portion of CBB or SCB (4/11 specimens)

Abbreviations: CAL, coracoacromial ligament; CBB, coracobrachial bursa; CP, coracoid process, SCB, subcoracoid bursa; SSB, subtendinous bursa of subscapularis.

[a]Of coracobrachialis and short head of biceps tendon.

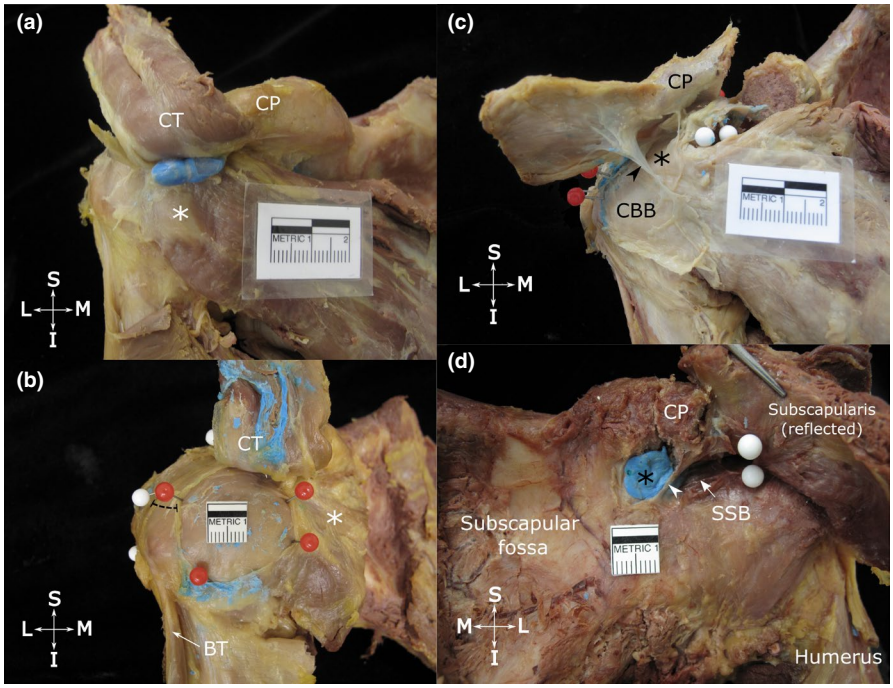

FIGURE 3 Location and dimensions of the coracobrachial (a and b) and subcoracoid bursa (c) and the relationship between the superior extension of the subtendinous bursa of subscapularis and the subcoracoid bursa (d). Anterior view of the shoulder showing (a) the typical location of the coracobrachial bursa (unopened, injected with blue latex), deep to the tip of the coracoid process (CP), conjoint tendon (CT, reflected superiorly) and overlying the subscapularis tendon (white asterisk); and (b) a large, circular coracobrachial bursa (opened, latex removed) with its floor exposed, delineated with red pins. The distance between the anterior boundary of the subacromial bursa (white pins) and lateral border of the coracobrachial bursa is indicated by the dashed line. (c) shows an opened subcoracoid bursa (black asterisk) that extends deep to the coracoid process (CP, resected and reflected superiorly) and shares a wall (arrowhead) with a coracobrachial bursa (CBB). (d) shows a subcoracoid bursa (filled with blue latex) and superior extension of the subtendinous bursa of subscapularis (SSB, arrow), separated by a thin wall (arrowhead). The attachment of the subtendinous bursa of subscapularis to the deep surface of the subscapularis tendon is indicated by white pins. Abbreviations: BT, biceps tendon (long head); I, inferior; L, lateral; M, medial; S, superior. Scale bar marked in cm

frequent distally (roof 44%, floor: 42%; Table S1). Differences in the distribution of the type of synovium were not statistically significant.

3.6 | Neurovascular structures of the shoulder bursae

From the 47 samples, 69 sections were included in the analysis (blood vessels $n = 43$; nerves $n = 26$), with 24 sections excluded due to tissue damage or lack of immunoreactivity to the neurofilament stain. The mean area of the ROI on the sections for blood vessel and nerve analysis was 2.6 ± 1.7 mm^2 (range 0.2–7.6 mm^2) and 3.4 ± 2.1 mm^2 (range 0.4–7.6 mm^2) respectively. The results of the blood vessel density are summarised in Table 4.

3.7 | Blood vessel density

Blood vessels were located in every sample. Small vessels were frequently present in the intima just below the synovial surface, with larger vessels present in the subintima (Figure 6). The blood vessel density was highest in the roofs of the SSB and the SAB (4.9% and 3.4% respectively), and lowest in the SAB floor (1.8%) and the CBB roof and floor (both 1.6%). A significantly higher blood vessel density was found in the SSB roof compared to the CBB roof ($p = 0.014$, 95% confidence interval). The remaining comparisons were not statistically significant.

3.8 | Neural structures

Twenty-six (60.5%) of the sections showed positive immunoreactivity to neurofilament and in 15 (57.7%) of these, neural structures were observed in the ROI (intima and subintima) of all of the different bursae. In the remaining 11 samples (42.3%), neural structures were only located deep into the ROI.

In the intima and subintima, free nerve endings and nerve bundles were identified (Figure 7). While free nerve endings were numerous and present in all but one sample, nerve bundles were less common (present in 6 of 15 samples). Encapsulated receptors were not identified in the ROI.

Neural structures were usually observed in areolar-adipose synovium, and less commonly in fibrous synovium. While the intimal layer itself appeared free of nerves, most neural structures were situated in the subintima in the same tissue layers as blood

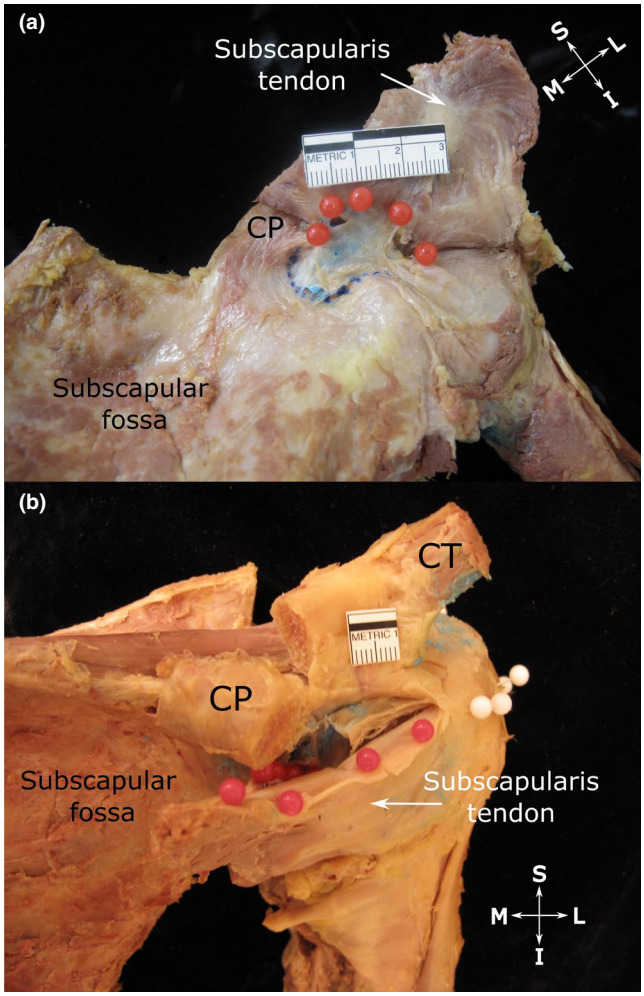

FIGURE 4 Subtendinous bursa of subscapularis (a) and extent of its superior extension along the anterior surface of the subscapularis tendon (b). (a) Anterior view of the shoulder showing the subtendinous bursa of subscapularis (injected with blue latex). Its roof (indicated by red pins) attaches to the upper aspect of the deep surface of the subscapularis tendon and its floor (indicated by blue dotted line) fuses with the neck of the scapula and root of the coracoid process (CP, tip resected) as well as the anterior glenohumeral joint capsule. (b) Anterosuperior view of the shoulder showing the subtendinous bursa of subscapularis, overhanging the upper edge of the subscapularis tendon and attaching to its superficial surface (indicated by red pins). The close relationship between the upper edge of the subscapularis tendon along with its bursal attachment to the underside of the coracoid process (CP, tip resected and reflected) is also visible. White pins indicate the extent of the subacromial bursa, but are not relevant to this image. Abbreviations: I, inferior; L, lateral; M, medial; S, superior. Scale bar marked in cm

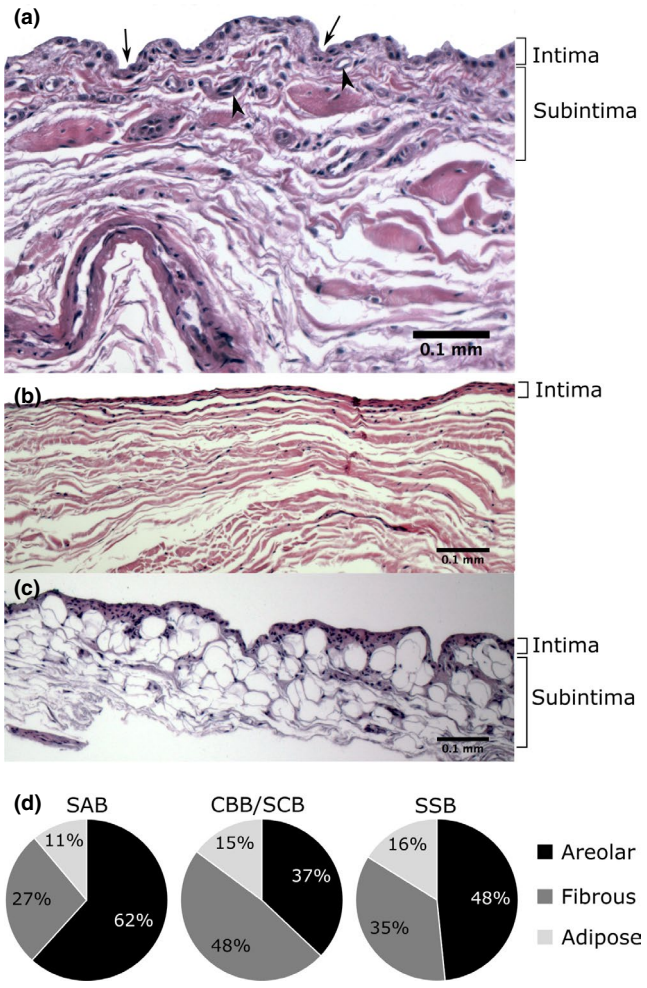

FIGURE 5 Types of bursal synovium (a–c) and its distribution in the various bursae (d). (a) Areolar and (b) fibrous synovium in the roof of the subacromial bursa, and (c) adipose synovium in the floor of the subacromial bursa; haematoxylin and eosin stain. (d) CBB/SCB: coracobrachial and subcoracoid bursa (combined values), $n = 27$ samples; SAB: subacromial bursa, $n = 81$ samples; SSB: subtendinous bursa of subscapularis, $n = 31$ samples

vessels, some distinctly contributing to neurovascular bundles. Neural structures within the ROI were localised to an average depth of 0.20 ± 0.13 mm (range 0.02–0.47 mm), with free nerve endings being identified more superficially than nerve bundles (mean depth 0.18 ± 0.13 mm, range 0.02–0.47 mm and 0.25 ± 0.10 mm, range 0.08–0.38 mm respectively).

In 19 of the samples, neural structures were present deep to the ROI. Free nerve endings were present in 18 (94.7%) and other nerve structures were located in 14 (73.7%) samples. These included larger nerve bundles and nerve structures resembling encapsulated mechanoreceptors, such as Pacinian and Golgi-Mazzoni corpuscles (Figure 8). Nerve structures tended to be more numerous and larger deep to the subintima.

4 | DISCUSSION

This study provides a comprehensive description of the morphology and histological characteristics of the SAB and related shoulder bursae in the subcoracoid region. Four types of bursae were identified in the anterolateral shoulder region. With the exception of one small communication between a SAB and CBB, the bursae in this region did not communicate despite their close proximity.

4.1 | Subacromial bursa

In adults, the SAB consistently extends both deep to the acromion and the deltoid muscle. Furthermore, the SAB displays a continuous subdeltoid portion that is normally not distinct or separate. This study did not confirm a subcoracoid portion of the SAB, insofar as—with the humerus in neutral position—the SAB did not reach deep to the coracoid process anteromedially. This contrasts with reports describing a constant or inconstant (37%) subcoracoid portion of the SAB (Codman, 1934; Mitchell et al., 1988; Pfuhl, 1934; Strizak et al., 1982).

The presence of a separate SDB as a rare finding (in 6% of cases) supports previous studies of full-term fetuses and adults, reporting SDB in 2.5% (Whittaker, 1910) and 6% (Strizak et al., 1982) respectively. However, this differs to dissection papers (Birnbaum & Lierse, 1992; Duranthon & Gagey, 2001; Seo et al., 2018) that describe a separate SDB in 79%–100% of specimens. Reasons for the differences in the occurrence of the SDB might be due to variations of dissection technique (Duranthon & Gagey, 2001; Seo et al., 2018) and/or the presence of bursal adhesions and plicae that may lead to partial or complete separation of bursal portions (Birnbaum & Lierse, 1992; Codman, 1934; Funk et al., 2006; Horwitz & Tocantins, 1938).

Variations in terminology for the shoulder bursae are evident in the literature (Kennedy et al., 2017). The term 'subacromial bursa' has been advocated by some authors based on developmental observations that the SAB originates underneath the acromion (Black, 1934; Gardner & Gray, 1953). However, the anatomical observations in this study do not justify the sole use of 'subacromial' over 'subdeltoid', and rather support the term 'subacromial-subdeltoid' bursa (Hochberg et al., 2011; Pansky & Gest, 2012; Rosse & Gaddum-Rosse, 1997).

These findings show that the attachment of the SAB roof is extensive, encompassing between the anterior third to the whole acromial length and over 70% of the coracoacromial ligament length, comparable

TABLE 4 Blood vessel density for all bursal locations

Sample location	Blood vessel density, median (%, IQR), number samples (*n*)
All samples	3.0 (1.6–4.8), (*n* = 43)
SAB roof	3.4 (1.9–4.6), (*n* = 13)
Proximal[a]	3.9 (2.7–6.2), (*n* = 9)
Distal[b]	1.9 (0.8–3.5), (*n* = 4)
SAB floor	1.8 (1.1–3.2), (*n* = 11)
CBB roof	1.6 (1.1–2.4), (*n* = 6)
CBB floor	1.6 (1.4–4.6), (*n* = 5)
SSB roof	4.9 (3.2–5.6), (*n* = 8)

Abbreviations: CBB, coracobrachial bursa; IQR, interquartile range; SAB, subacromial bursa; SSB, subtendinous bursa of subscapularis.

[a]Deep to the acromion or coracoacromial ligament and 5–10 mm distal to the acromion or coracoacromial ligament.

[b]5–10 mm proximal to or covering the greater tubercle.

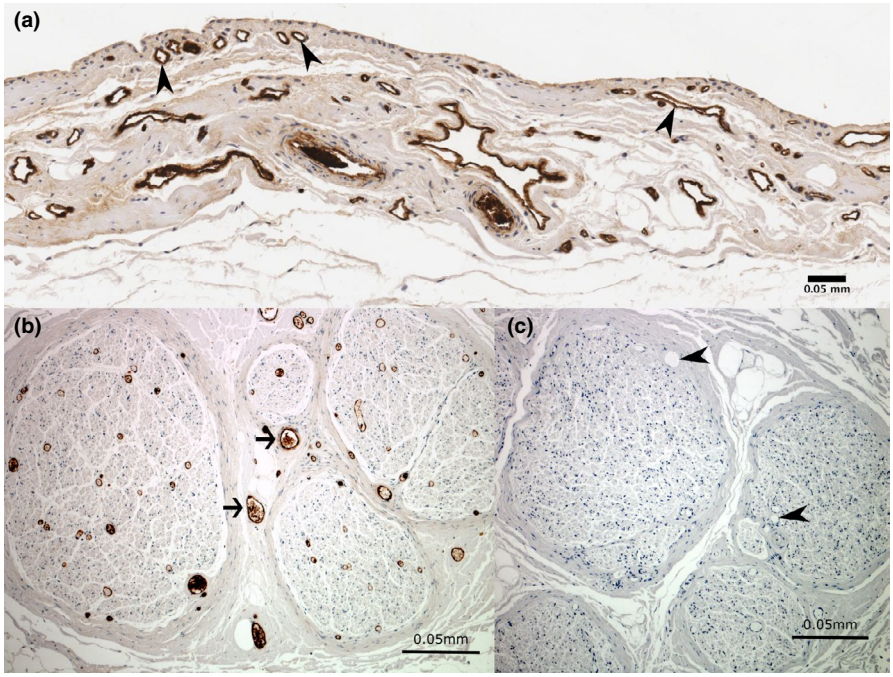

FIGURE 6 Immunoreactivity for von Willebrand factor showing blood vessels in the (a) subacromial bursa and (b) positive control tissue. Sections showing immunoreactivity to von Willebrand factor in (a) blood vessels in the subacromial bursa (arrowheads) and (b) blood vessels (arrows) in the positive control section within the sciatic nerve. The negative control section (c) shows no immunoreactivity to von Willebrand factor in blood vessels (arrowheads) or other non-specific staining. Cell nuclei are stained blue (haematoxylin)

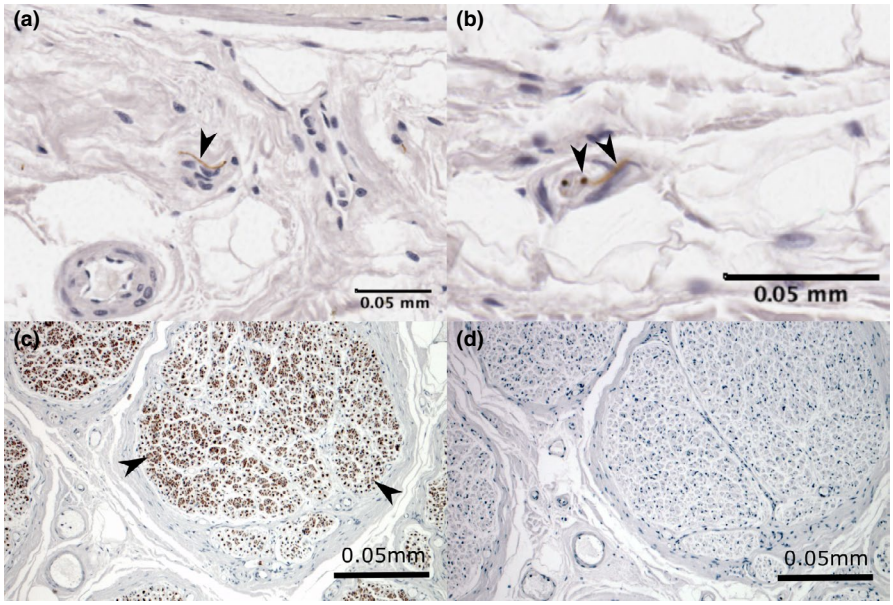

FIGURE 7 Immunoreactivity for neurofilament showing neural tissue in (a and b) bursal and (c) positive control tissue. Sections showing free nerve endings (arrowheads) within the (a) coracobrachial bursa floor and (b) subacromial bursa roof and (c) nerve bundles (arrowheads) in the positive control within the sciatic nerve. The negative control (d) shows no immunoreactivity to neurofilament or other non-specific staining. Cell nuclei are stained blue (haematoxylin)

to descriptive studies (Birnbaum & Lierse, 1992; Codman, 1934; Cooper et al., 1993; Duranthon & Gagey, 2001; Mitchell et al., 1988; Pfuhl, 1934). The extent of the SAB roof along the acromion (2.9 ± 1.0 cm) also corresponds with data (2.8 ± 0.6 cm) from Beals et al. (1998) which is the only other publication that has quantified this measurement. Furthermore, the SAB roof displayed a constant firm attachment to the overlying subdeltoid fascia, with deltoid fibres blending with the fascia in the vicinity of the anterolateral aspect of the humeral head in almost a third of specimens, confirming observations (in up 50% of cases) of two cadaver studies (Birnbaum et al., 1998; Codman, 1934).

Kinematic studies of cadaveric shoulders have described that the lateral portion of the SAB roof slides underneath its medial portion creating a fold on top of each other in the subacromial space, at about 90–100˚of abduction (Birnbaum & Lierse, 1992; Birnbaum et al., 1998; Codman, 1934). Several features of the SAB roof attachment presented in this research may contribute to, and allow for this movement. The acromial and coracoacromial ligament attachments are thought to stretch the SAB roof along the coracoacromial arch (Birnbaum & Lierse, 1992; Birnbaum et al., 1998). In addition, the firm attachment of the SAB roof to the subdeltoid fascia has been proposed to function like a restraint, thereby limiting movement of the roof in this area, and enabling the lateral roof to glide beneath the acromion. The deltoid muscle fibres which insert into the SAB subdeltoid fascia are further hypothesised to contribute to the control of bursal movement during shoulder abduction, by lifting the SAB roof to avoid entrapment underneath the acromion (Birnbaum & Lierse, 1992; Birnbaum et al., 1998). This mechanism could be likened to the relationship of the articularis genus muscle and suprapatellar bursa in the knee (Grob et al., 2017). However, functional studies are needed to establish the role of deltoid and the subdeltoid fascia on the SAB.

The SAB floor dimensions are comparable with the findings of Birnbaum and Lierse (1992), but Seo et al. (2018) reported smaller values. As previously described (Beals et al., 1998; Birnbaum & Lierse, 1992; Codman, 1934; Mitchell et al., 1988; Pfuhl, 1934), the SAB floor was usually fused with the whole width of the underlying supraspinatus tendon and the greater tubercle. This firm connection indicates that separate movement between the two layers does not occur. Instead, it suggests that the SAB is displaced simultaneously with the tendon and shoulder capsule with movement, for example the bursa moves medially with shoulder abduction (Birnbaum & Lierse, 1992).

The SAB floor may extend medial to the coracoacromial ligament, the acromioclavicular joint (in 69%) and the acromion overlying the supraspinatus muscle. A similar prevalence (73%) of the SAB extending underneath or medial to the acromioclavicular joint has been reported in the literature (Beals et al., 1998; Birnbaum & Lierse, 1992; Codman, 1934; Mitchell et al., 1988; Pfuhl, 1934). The lateral extent distal to the greater tubercle for up to 2 cm, is similar to that reported in a historical publication (Fick, 1904; approximated mean value of 2.0 cm), but smaller than in another recent paper (3.2 ± 1.5 cm; Seo et al., 2018). Anteromedially, the SAB is commonly bounded by the lesser tubercle and usually does not extend distal to the transverse humeral ligament. However, it is important to consider that the lesser tubercle might instead be covered by a CBB. These findings emphasise the large area that may be occupied by the SAB, which is a relevant consideration for imaging and interventions that use these bony landmarks for orientation (e.g. injections and acupuncture needling; Cook, 2011; Feigl et al., 2007; Peuker & Cummings, 2003; Tallia & Cardone, 2003). Particularly, the lateral bursal extent is important to consider to ensure complete assessment of the SAB on imaging and to

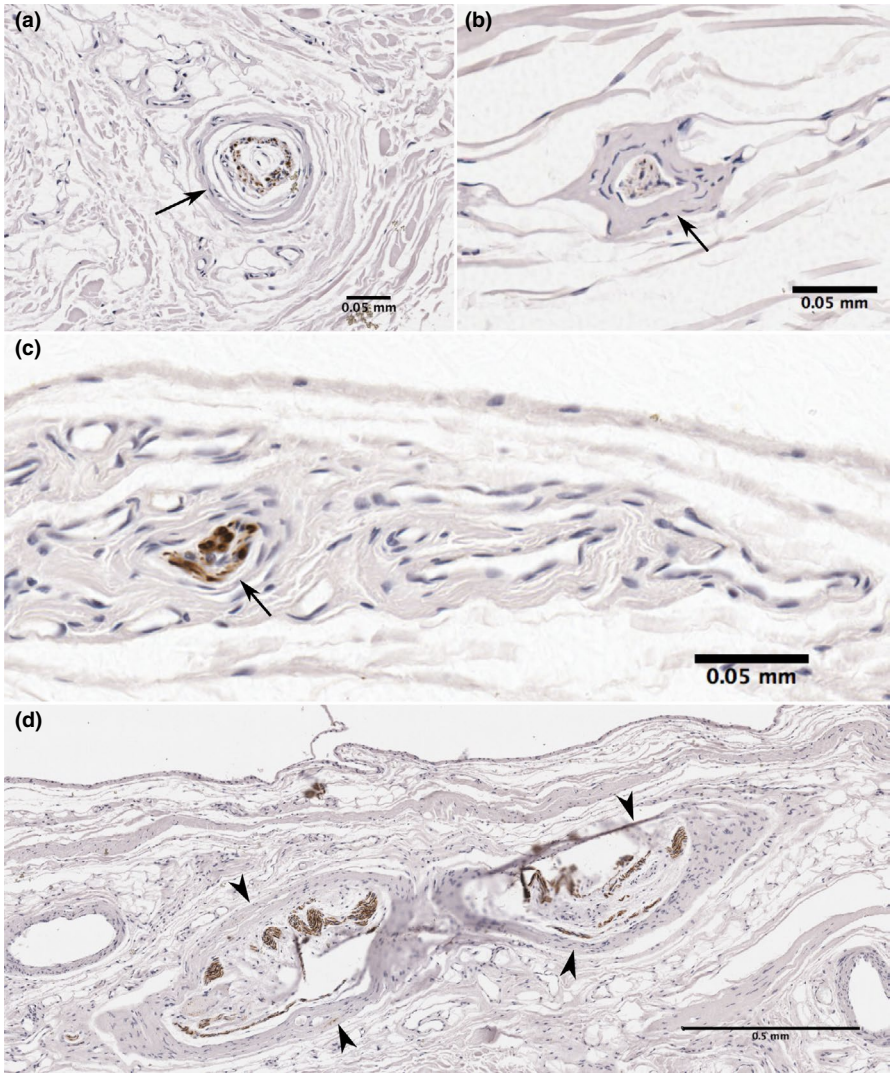

FIGURE 8 Neural structures in the subacromial and coracobrachial bursa deep to the subintima. Sections showing immunoreactivity for neurofilament contain large encapsulated neural structure resembling a (a, b) Pacinian corpuscle with typical onion-like multi-layered capsule. Central axons show immunoreactivity to neurofilament, (c) large nerve bundle and (d) Golgi-Mazzoni corpuscles just deep to the subintima. Sections obtained from (a) subacromial bursa floor, (b, c) subacromial bursa roof, (d) coracobrachial bursa floor

spare the bursa when administering injections or vaccines into the deltoid muscle (Beals et al., 1998; Cooper et al., 1993; Duranthon & Gagey, 2001; Nottage, 1993).

Similarly, awareness of the course of the axillary nerve is important clinically in order to avoid iatrogenic injury (Apaydin et al., 2007; Beals et al., 1998; Gadea et al., 2015; Nottage, 2018). The results suggest that the inferior extent of the SAB courses proximally to the anterior branch of the axillary nerve, as previously described (Beals et al., 1998; Duranthon & Gagey, 2001).

4.2 | Coracobrachial and subcoracoid bursae

The bursae in the subcoracoid space are distinct structures, although variable in terms of constancy and size. The CBB was a separate structure, present in 94% of specimens, which is consistent with a seminal cadaver study of 100 shoulders (Horwitz & Tocantins, 1938) but higher than reported in another study of 11 shoulders (64%; Pfuhl, 1934). As with previous descriptions (Colas et al., 2004; Fick, 1904; Pfuhl, 1934), the SCB was smaller than the CBB and inconstant, present in 31% of specimens. A close relationship and potential connection were observed between the posterior border of the CBB and anterior border of the SAB, a finding which supports that of Horwitz and Tocantins (1938) who reported a certain degree of overlap between these two bursae in 13% of cases. These authors also found that the CBB and SAB communicated in 12% of specimens, yet in the present study this was confirmed in one (6%) specimen. Therefore, the data suggest that while the SAB and CBB might come into close contact with each other, communication appears to occur rarely.

4.3 | Subtendinous bursa of subscapularis

The SSB is the only bursa that communicates with the glenohumeral joint capsule under physiological conditions (DePalma et al., 1949). In this study, the SSB was constant and communicated with the anterior capsule (94% of specimens), in agreement with reported data relating to constancy (88%–100%) and communication (74%–96%; Colas et al., 2004; DePalma et al., 1949; Gong et al., 2017; Horwitz & Tocantins, 1938; Moseley & Övergaard, 1962; Schraner & Major, 1999; Steinbeck et al., 1998). The dimensions of the SSB lay within the ranges reported by Horwitz and Tocantins (1938) (1.25–3.75 cm) but were smaller than those described by Colas et al. (2004). Determining the dimensions of the SSB was the most difficult of all the investigated bursae because of the concealed location of the bursa and the bursal configuration.

A superior portion of the SSB projecting superior to the upper edge of the subscapularis tendon was observed in 81% of specimens. Colas et al. (2004) reported this superior extension protruding deep to the root of the coracoid in 36% of specimens, when the SSB was distended with saline. They interpreted this extension as a continuation of the SSB and a communication with the SCB. Furthermore, they argued that the SSB replaced the SCB in these cases. This is in contrast to the present study, in which the SSB came into close contact with a SCB or a CBB in more than 50% of the specimens.

In nearly two-thirds of specimens, the SSB extended along and overhung the upper edge of the subscapularis tendon and attached to its anterior surface, which is consistent with published data (Moseley & Övergaard, 1962). The overhang of the bursa has been previously described as both a normal and pathological feature of the SSB (Codman, 1934; Fick, 1904; Grainger et al., 2000; Horwitz & Tocantins, 1938). In the present study, SSB overhang was not associated with subscapularis pathology suggesting this is a normal finding. Clinically, it is important to be aware of the superior portion of the SSB and its potential extent anteriorly to the subscapularis tendon to avoid confusion with CBB or SCB in the area, for example in shoulder imaging (Grainger et al., 2000; Schraner & Major, 1999).

In summary, there may be three separate bursal structures in the small anatomical space between the coracoid process and the upper edge of the subscapularis tendon—the superior extension of the SSB with its anterior overhang, the SCB and CBB. This arrangement suggests that the subcoracoid space is subject to various stresses and friction during shoulder movement, occurring particularly between the root and deep surface of the coracoid process and the tendons of subscapularis, coracobrachialis and short head of biceps.

4.4 | Type and distribution of synovium

Areolar synovium was the most prevalent in the shoulder bursae, consistent with other regions including the knee and gluteal bursae (43%–59%; Castor, 1960; Woodley et al., 2008). These findings support Key's (1932) proposition that areolar synovium may be regarded as the typical type of synovial tissue, which is usually present in areas that are not subjected to pressure or strain, and where joint function causes movement on the underlying tissue. The surface of synovium, particularly the areolar type, may display crimps and folds that disappear when stretched, contributing to the range of bursal movement during shoulder movements (Smith, 2011). This could mean that bursal areas that possess a higher proportion of synovium with uneven surfaces, for example the areolar type, might be able to facilitate more movement compared to straight synovial surfaces.

It was observed that all bursal roofs tended to be composed of areolar rather than fibrous synovium, while the reverse was seen in the floors. Furthermore, the SAB roof displayed a decrease in areolar synovium and increase in fibrous synovium from proximal to distal. While these findings did not reach statistical significance, it appears that synovial morphology varies within the bursae depending on anatomical location, suggesting potential functional differences between regions. For example the proximal roof of the SAB may be subject to less pressure and be more mobile compared to the floor. The relatively high proportion of fibrous synovium in the CBB and SCB (48%) suggests they may be exposed to increased forces in the subcoracoid space, as in joints, this type of synovium typically covers areas subjected to higher pressure and strain (Key, 1932; Smith, 2011). Increased forces on the bursae in the subcoracoid space might be dependent on orientation of the subscapularis tendon and the overlying tip of the coracoid process and conjoint tendon, and have been found to vary with shoulder position (Colas et al., 2004; Hughes et al., 2012).

4.5 | Blood vessel density

Compared to the median blood vessel density of all bursae combined, the roofs of the SSB and SAB tended to have a higher vascularity than the floor of the SAB and the roof and floor of the CBB. Variation in blood vessel density depending on the type of synovial tissue has been reported in joint synovium, with areolar synovium being the most vascular (Castor, 1960; Key, 1932; Wilkinson & Edwards, 1989). This study confirmed variations in blood vessel density dependent on bursal location with the SSB roof displaying a significantly higher density compared to the CBB roof. These findings may imply variable functions of bursal regions depending on blood vessel density. For example areas with higher vascularity could serve to distribute blood supply and nutrition into less well vascularised bursal areas and might be more active in secreting and absorbing synovial fluid. The blood vessels may also contribute to the provision of nutrients to cells involved in the tissue remodelling of surrounding structures. This supports propositions regarding the potential of the SAB to contribute to rotator cuff tendon healing (Chillemi et al., 2011; Gartsman, 2001; Hyvönen et al., 2003; Ishii et al., 1997; Uhthoff & Sarkar, 1991). The SAB floor and its distal roof were among the least vascular areas (1.8% and 1.9% respectively). These areas correspond anatomically with the 'critical zone' of hypovascularity of

the insertional tendinous portion of the rotator cuff (particularly supraspinatus) in which tears commonly occur (Lohr & Uhthoff, 1990; Naidoo et al., 2016; Rathbun & Macnab, 1970; Yepes et al., 2007). A diminished blood supply in these areas might negatively influence healing of the surrounding tissues, particularly the distal supraspinatus tendon.

4.6 | Neural structures

The neural structures identified in the subintima of all the examined bursal areas confirm previous accounts that portray the SAB as a well-innervated structure, and demonstrate innervation of the CBB and SSB. The data suggest that all of the examined bursae contribute to nociception of the shoulder (Ide et al., 1996; Soifer et al., 1996; Tomita et al., 1997; Vangsness et al., 1995). Although the aetiology of shoulder pain is uncertain, it may be due to a reduction in the dimensions of the subacromial or subcoracoid spaces, with subsequent compression or irritation of the intervening bursae and tendons (Friedman et al., 1998; Lewis, 2009; Radas & Pieper, 2004; Seitz & Michener, 2011). In contrast to previous reports (Ide et al., 1996; Tomita et al., 1997; Vangsness et al., 1995) of mechanoreceptors and unclassified receptors in the SAB (roof), this study found only encapsulated structures resembling mechanoreceptors deep to the subintima—these included Golgi Mazzoni [high-threshold, slow adapting, responding to considerable stresses when joints are at the extremes of their range of movement] and Pacinian [low-threshold, rapid-adapting, responding to sudden changes in mechanical stress, such as joint acceleration and deceleration] corpuscles (Freeman & Wyke, 1967; Witherspoon et al., 2014; Zimny, 1988). It is possible that other shoulder structures are more important for proprioception than the SAB, with a range of mechanoreceptors also identified in surrounding tissues including the coracoacromial, coracoclavicular and acromioclavicular ligaments, as well as the glenohumeral capsule and labrum (Hashimoto et al., 1994; Morisawa, 1998; Vangsness et al., 1995; Witherspoon et al., 2014 #1041).

Future three-dimensional investigation of neural structures is warranted to determine the distribution and location of different nerve endings across the different bursae across a spectrum of shoulders, including those with known pathology. This would improve our understanding of their function, including their contribution to both nociception and proprioception of the shoulder.

4.7 | Limitations

This study has some limitations that require consideration. The relatively small sample size impedes comparisons regarding age, side and sex. Given that all donors in this study were over 67 years of age, degenerative changes in the rotator cuff were not unexpected, and consistent with findings of anatomical studies (Hijioka et al., 1993; Horwitz, 1939; Ogata & Uhthoff, 1990). However, this reduces the generalisability of the results to younger and healthy individuals. The cadavers' age possibly affected the quantitative results of the neurovascular examination, because ageing has been associated with a decline of peripheral nerve fibres and mechanoreceptors and potential alterations of blood vessels (Jani & Rajkumar, 2006; Morisawa, 1998; Rein et al., 2013; Verdú et al., 2000). In addition, the lumen of blood vessels might have been influenced (by shrinkage, collapse or swelling) occurring during embalming and histological processing, or proliferation of endothelial cells due to underlying pathology, thereby contributing to over- or under-estimation of density calculations (Sarkar & Uhthoff, 1983; Suvarna et al., 2013). Furthermore, the level of inflammation of the synovium was not assessed in the histological samples and incorporating the use of a synovitis score would have offered more information about potential inflammatory changes (Krenn et al., 2006). It would be useful to compare the findings of this study with a detailed examination of shoulder bursae in younger people, for example by using surgical samples.

Just over one-third of the sections in the present study did not show immunoreactivity to neurofilament. These results suggest that no nerves were present in the respective samples, since immunoreactivity to neurofilament was consistently present in the positive control sections. Other potential reasons for a lack of immunoreactivity in the present samples include ineffective staining of the bursal samples, issues with tissue fixation or technical difficulties during processing, and use of a single antibody rather than a combination of stains (which made it difficult to confirm the presence/absence of Ruffini corpuscles; Rein et al., 2013). It could be argued that the density of neural tissue reported in the present study would be smaller if all sections, irrespective of their evidence of immunoreactivity, had been included in the analysis.

5 | CONCLUSION

The consistent findings regarding SAB attachments to both the acromion as well as the subdeltoid fascia, support the use of the term subacromial-subdeltoid bursa. Similarly, the constant relationship of the CBB to both the tip of the coracoid process and the conjoint tendon on the one hand, as well as the confinement of the SCB deep to the coracoid process, validates discriminating between the CBB and SCB. These findings question the common existence of a separate SDB, and provide new information regarding the distinctness of bursae related to the coracoid process.

The location and attachment sites of the investigated bursae along with the variations of the type of synovial tissue and the density of vascular structures indicate differences between the shoulder bursae and between the regions of each bursa. Fixed and mobile portions of the SAB and related shoulder bursae enable movement in relation to the surrounding structures. Variations in the type of bursal synovium may further reflect differences between bursal location and function. The presence of neurovascular structures demonstrates that these bursae have the potential

to contribute blood supply to surrounding structures and are involved in mechanoreception. The potential roles of shoulder bursae are relevant for shoulder function and are important to consider in clinical situations, particularly during and following surgery. Given the relative proximity of all four of these bursae, detailed morphological descriptions are essential to assist in accurately locating these structures, whether it be during surgery, image analysis, injection or palpation.

ACKNOWLEDGEMENTS

The authors sincerely thank those individuals and their families who donated their bodies to science for the purpose of anatomical research. We thank the staff of the Histology Services Unit, Department of Pathology, University of Otago, New Zealand for their assistance with the histological techniques, sonographer Jillian Muirhead for injecting the bursae under ultrasound guidance, and Robert McPhee for his assistance with some of the illustrations included in this paper.

AUTHORS' CONTRIBUTION

M.S.K.: Study design, dissections, histological techniques, data collection and analysis, photomicrographs, drafting and editing of the manuscript. H.D.N.: Study design, supervision of the work, data analysis, commenting and editing of drafts and the final version of the manuscript. S.J.W.: Study design, supervision of the work, data analysis, commenting and editing of drafts and the final version of the manuscript.

DATA AVAILABILITY STATEMENT

The data that support the findings of this study are available from the corresponding author upon reasonable request.

ORCID

Marion S. Kennedy https://orcid.org/0000-0001-8650-1321
Helen D. Nicholson https://orcid.org/0000-0003-0921-2758
Stephanie J. Woodley https://orcid.org/0000-0002-7288-0209

REFERENCES

Apaydin, N., Uz, A., Bozkurt, M. & Elhan, A. (2007) The anatomic relationships of the axillary nerve and surgical landmarks for its localization from the anterior aspect of the shoulder. *Clinical Anatomy*, 20(3), 273–277.

Beals, T.C., Harryman, D.T. & Lazarus, M.D. (1998) Useful boundaries of the subacromial bursa. *Arthroscopy*, 14(5), 465–470.

Birnbaum, K. & Lierse, W. (1992) Anatomy and function of the bursa subacromialis. *Acta Anatomica*, 145(4), 354–363.

Birnbaum, K., Prescher, A. & Heller, K.D. (1998) Anatomic and functional aspects of the kinetics of the shoulder joint capsule and the subacromial bursa. *Surgical and Radiologic Anatomy*, 20(1), 41–45.

Black, B.M. (1934) The prenatal incidence, structure and development of some human synovial bursae. *The Anatomical Record*, 60(3), 333–355.

Blaine, T.A., Kim, Y.-S., Voloshin, I., Chen, D., Murakami, K., Chang, S.-S. et al. (2005) The molecular pathophysiology of subacromial bursitis in rotator cuff disease. *Journal of Shoulder and Elbow Surgery*, 14(1), S84–S89.

Brooks, C., Revell, W. & Heatley, F. (1992) A quantitative histological study of the vascularity of the rotator cuff tendon. *The Journal of Bone and Joint Surgery*, 74-B(1), 151–153.

Cadogan, A., Laslett, M., Hing, W.A., McNair, P.J. & Coates, M.H. (2011) A prospective study of shoulder pain in primary care: prevalence of imaged pathology and response to guided diagnostic blocks. *BMC Musculoskeletal Disorders*, 12(1), 119–136.

Castor, C.W. (1960) The microscopic structure of normal human synovial tissue. *Arthritis & Rheumatism*, 3(2), 140–151.

Chillemi, C., Petrozza, V., Franceschini, V., Garro, L., Pacchiarotti, A., Porta, N. et al. (2016) The role of tendon and subacromial bursa in rotator cuff tear pain: a clinical and histopathological study. *Knee Surgery, Sports Traumatology, Arthroscopy*, 24(12), 3779–3786.

Chillemi, C., Petrozza, V., Garro, L., Sardella, B., Diotallevi, R., Ferrara, A. et al. (2011) Rotator cuff re-tear or non-healing: histopathological aspects and predictive factors. *Knee Surgery, Sports Traumatology, Arthroscopy*, 19(9), 1588–1596.

Codman, E.A. (1934) *The shoulder: rupture of the supraspinatus tendon and other lesions in or about the subacromial bursa*. Thomas Todd Co.

Colas, F., Nevoux, J. & Gagey, O. (2004) The subscapular and subcoracoid bursae: descriptive and functional anatomy. *Journal of Shoulder and Elbow Surgery*, 13(4), 454–458.

Cook, I.F. (2011) An evidence based protocol for the prevention of upper arm injury related to vaccine administration (UAIRVA). *Human Vaccines*, 7(8), 845–848.

Cooper, D.E., O'Brien, S.J. & Warren, R.F. (1993) Supporting layers of the glenohumeral joint. An anatomic study. *Clinical Orthopaedics & Related Research*, 289, 144–155.

DePalma, A.F., Callery, G. & Bennett, G.A. (1949) Shoulder joint: variational anatomy and degenerative regions of the shoulder joint. *Instructional Course Lectures*, 6, 255–281.

Determe, D., Rongières, M., Kany, J., Glasson, J.M., Bellumore, Y., Mansat, M. et al. (1996) Anatomic study of the tendinous rotator cuff of the shoulder. *Surgical and Radiologic Anatomy*, 18(3), 195–200.

Djade, C.D., Porgo, T.V., Zomahoun, H.T.V., Perrault-Sullivan, G. & Dionne, C.E. (2020) Incidence of shoulder pain in 40 years old and over and associated factors: a systematic review. *European Journal of Pain*, 24(1), 39–50.

Drakes, S., Thomas, S., Kim, S., Guerrero, L. & Lee, S.W. (2015) Ultrasonography of subcoracoid bursal impingement syndrome. *PM & R: The Journal of Injury, Function, and Rehabilitation*, 7, 329–333.

Dunn, T., Heller, C.A., McCarthy, S.W. & Dos Remedios, C. (2003) Anatomical study of the "trochanteric bursa". *Clinical Anatomy*, 16(3), 233–240.

Duranthon, L.D. & Gagey, O.J. (2001) Anatomy and function of the subdeltoid bursa. *Surgical & Radiologic Anatomy*, 23(1), 23–25.

Federative International Programme for Anatomical Terminology (FIPAT). (2019) *Terminologia Anatomica*, 2nd edition. Terminologia Anatomica. FIPAT.library.dal.ca. Federative International Programme for Anatomical Terminology. https://fipat.library.dal.ca/ta2/

Feigl, G.C., Anderhuber, F., Dorn, C., Pipam, W., Rosmarin, W. & Likar, R. (2007) Modified lateral block of the suprascapular nerve: a safe approach and how much to inject? A morphological study. *Regional Anesthesia and Pain Medicine*, 32(6), 488–494.

Feldman, M.D. (2018) When less is more—the benefits of limiting bursectomy in arthroscopic rotator cuff repair. *Arthroscopy*, 34(12), 3175–3176.

Fick, R. (1904) Handbuch der Anatomie und Mechanik der Gelenke. In: von Bardeleben, K. (Ed.) *Handbuch der Anatomie des Menschen*. Gustav Fischer.

Field, A.P. (2013) *Discovering statistics using IBM SPSS statistics*, 4th edition. Sage.

Firestein, G.S., Gabriel, S.E., McInnes, I.B. & O'Dell, J.R. (2017) *Kelley and Firestein's textbook of rheumatology*, 10th edition. Elsevier.

Freeman, M.A. & Wyke, B. (1967) The innervation of the knee joint. An anatomical and histological study in the cat. *Journal of Anatomy*, 101(3), 505–532.

Fremerey, R., Bastian, L. & Siebert, W.E. (2000) The coracoacromial ligament: anatomical and biomechanical properties with respect to age and rotator cuff disease. *Knee Surgery, Sports Traumatology, Arthroscopy*, 8(5), 309–313.

Friedman, R.J., Bonutti, P.M. & Genez, B. (1998) Cine magnetic resonance imaging of the subcoracoid region. *Orthopedics*, 21(5), 545–548.

Funk, L., Levy, O., Even, T. & Copeland, S.A. (2006) Subacromial plica as a cause of impingement in the shoulder. *Journal of Shoulder and Elbow Surgery*, 15(6), 697–700.

Gadea, F., Bouju, Y., Berhouet, J., Bacle, G. & Favard, L. (2015) Deltopectoral approach for shoulder arthroplasty: anatomic basis. *International Orthopaedics*, 39(2), 215–225.

Gardner, E. & Gray, D.J. (1953) Prenatal development of the human shoulder and acromioclavicular joints. *American Journal of Anatomy*, 92(2), 219–276.

Gartsman, G.M. (2001) Arthroscopic rotator cuff repair. *Clinical Orthopaedics and Related Research*, 390, 95–106.

Gong, J.-C., Chen, N.A., Chen, J.-F., Xu, Z., Wu, Y.I., Li, J.-Q. et al. (2017) Subscapular bursa: anatomy and magnetic resonance appearance. *Chinese Medical Journal*, 130(4), 1739–1740.

Grainger, A.J., Tirman, P.F.J., Elliott, J.M., Kingzett-Taylor, A., Steinbach, L.S. & Genant, H.K. (2000) MR anatomy of the subcoracoid bursa and the association of subcoracoid effusion with tears of the anterior rotator cuff and the rotator interval. *American Journal of Roentgenology*, 174(5), 1377–1380.

Grob, K., Gilbey, H., Manestar, M., Ackland, T. & Kuster, M.S. (2017) The anatomy of the articularis genus muscle and its relation to the extensor apparatus of the knee. *JBJS Open Access*, 2(4), e0034.

Hall, M. & Richardson, T. (2016) Basic statistics for comparing categorical data from 2 or more groups. *Hospital Pediatrics*, 6(6), 383–385.

Hashimoto, T., Hamada, T., Sasaguri, Y. & Suzuki, K. (1994) Immunohistochemical approach for the investigation of nerve distribution in the shoulder joint capsule. *Clinical Orthopaedics and Related Research*, 305, 273–282.

Hijioka, A., Suzuki, K., Nakamura, T. & Hojo, T. (1993) Degenerative change and rotator cuff tears. *Archives of Orthopaedic and Trauma Surgery*, 112(2), 61–64.

Hill, C.L., Gill, T.K., Shanahan, E.M. & Taylor, A.W. (2010) Prevalence and correlates of shoulder pain and stiffness in a population-based study: The North West Adelaide Health Study. *International Journal of Rheumatic Diseases*, 13(3), 215–222.

Hirschmann, M.T., Zschabitz, A. & Stofft, E. (2007) Immunohistochemical characterization of human synovial bursa cells by light and transmission electron microscopy. Where do these cells come from? *International Journal of Morphology*, 25(1), 5–14.

Hochberg, M.C., Silman, A.J., Smolen, J.S. & Weisman, M.H. (2011) *Rheumatology*, 5th edition. Mosby Elsevier.

Horwitz, M. (1939) Lesions of the supraspinatus tendon and associated structures: investigation of comparable lesions in the hip joint. *Archives of Surgery*, 38(6), 990–1003.

Horwitz, M. & Tocantins, L.M. (1938) An anatomical study of the role of the long thoracic nerve and the related scapular bursae in the pathogenesis of local paralysis of the serratus anterior muscle. *The Anatomical Record*, 71(4), 375–385.

Hughes, P.C., Green, R.A. & Taylor, N.F. (2012) Measurement of subacromial impingement of the rotator cuff. *Journal of Science and Medicine in Sport*, 15(1), 2–7.

Hyvönen, P., Melkko, J., Lehto, V.P. & Jalovaara, P. (2003) Involvement of the subacromial bursa in impingement syndrome of the shoulder as judged by expression of tenascin-C and histopathology. *Journal of Bone and Joint Surgery*, 85-B, 299–305.

Ide, K., Shirai, Y., Ito, H. & Ito, H. (1996) Sensory nerve supply in the human subacromial bursa. *Journal of Shoulder and Elbow Surgery*, 5(5), 371–382.

Ishii, H., Brunet, J.A., Welsh, R.P. & Uhthoff, H.K. (1997) "Bursal reactions" in rotator cuff tearing, the impingement syndrome, and calcifying tendinitis. *Journal of Shoulder and Elbow Surgery*, 6(2), 131–136.

Jani, B. & Rajkumar, C. (2006) Ageing and vascular ageing. *Postgraduate Medical Journal*, 82(968), 357–362.

Kennedy, M.S., Nicholson, H.D. & Woodley, S.J. (2017) Clinical anatomy of the subacromial and related shoulder bursae: a review of the literature. *Clinical Anatomy*, 30(2), 213–226.

Key, J.A. (1932) The synovial membrane of joints and bursae. In: Cowdry, E.V. (Ed.) *Special cytology*. Hoeber: Paul B.

Kim, H.-Y. (2017) Statistical notes for clinical researchers: Chi-squared test and Fisher's exact test. *Restorative Dentistry & Endodontics*, 42(2), 152–155.

Krenn, V., Morawietz, L., Burmester, G.-R., Kinne, R.W., Mueller-Ladner, U., Muller, B. et al. (2006) Synovitis score: discrimination between chronic low-grade and high-grade synovitis. *Histopathology*, 49(4), 358–364.

Lewis, J.S. (2009) Rotator cuff tendinopathy. *British Journal of Sports Medicine*, 43(4), 236–241.

Lohr, J.F. & Uhthoff, H.K. (1990) The microvascular pattern of the supraspinatus tendon. *Clinical Orthopaedics & Related Research*, 254, 35–38.

Luime, J.J., Koes, B.W., Hendriksen, I., Burdorf, A., Verhagen, A.P., Miedema, H.S. et al. (2004) Prevalence and incidence of shoulder pain in the general population; a systematic review. *Scandinavian Journal of Rheumatology*, 33(2), 73–81.

Mathews, P.V. & Glousman, R.E. (2005) Accuracy of subacromial injection: anterolateral versus posterior approach. *Journal of Shoulder and Elbow Surgery*, 14(2), 145–148.

Mitchell, M.J., Causey, G., Berthoty, D.P., Sartoris, D.J. & Resnick, D. (1988) Peribursal fat plane of the shoulder: anatomic study and clinical experience. *Radiology*, 168(3), 699–704.

Molini, L., Mariacher, S. & Bianchi, S. (2012) US guided corticosteroid injection into the subacromial-subdeltoid bursa: technique and approach. *Journal of Ultrasound*, 15(1), 61–68.

Monro, A. (1799) *Alexander Monro's Abbildungen und Beschreibungen der Schleimsäcke des menschlichen Körpers*. Breitkopf und Härtel.

Moore, K.L. (2014) *Clinically oriented anatomy*, 7th edition. Wolters Kluwer/Lippincott Williams & Wilkins Health.

Morisawa, Y. (1998) Morphological study of mechanoreceptors on the coracoacromial ligament. *Journal of Orthopaedic Science*, 3(2), 102–110.

Moseley, H.F. & Övergaard, B. (1962) The anterior capsular mechanism in recurrent anterior dislocation of the shoulder. *The Journal of Bone and Joint Surgery*, 44-B(4), 913–927.

Naidoo, N., Lazarus, L. & Satyapal, K. (2016) The histological analysis of the glenohumeral "critical zone". *International Journal of Morphology*, 34(3), 1051–1057.

Nam, J.-H., Park, S., Lee, H.-R. & Kim, S.H. (2018) Outcomes after limited or extensive bursectomy during rotator cuff repair: randomized controlled trial. *Arthroscopy*, 34(12), 3167–3174.

Neer, C.S. (1983) Impingement lesions. *Clinical Orthopaedics and Related Research*, 173, 70–77.

Nottage, W.M. (1993) Arthroscopic anatomy of the glenohumeral joint and subacromial bursa. *Orthopedic Clinics of North America*, 24(1), 27–32.

Nottage, W.M. (2018) Shoulder anatomy, finding the axillary nerve: measure twice, cut once. *Arthroscopy*, 34(3), 804–805.

Ogata, S. & Uhthoff, H.K. (1990) Acromial enthesopathy and rotator cuff tear. A radiologic and histologic postmortem investigation of the coracoacromial arch. *Clinical Orthopaedics and Related Research*, 254, 39–48.

Pan, J., Dinh, T.T., Rajaraman, A., Lee, M., Scholz, A., Czupalla, C.J. et al. (2016) Patterns of expression of factor VIII and von Willebrand factor by endothelial cell subsets in vivo. *Blood*, 128(1), 104–109.

Pansky, B. & Gest, T.R. (2012) *Lippincott's concise illustrated anatomy. Volume 1, Back, upper limb & lower limb*, 1st edition. Wolter Kluwer/Lippincourt Williams & Wilkins.

Perumal, V., Woodley, S.J. & Nicholson, H.D. (2019) Neurovascular structures of the ligament of the head of femur. *Journal of Anatomy*, 234(6), 778–786.

Peuker, E. & Cummings, M. (2003) Anatomy for the acupuncturist – facts & fiction. 3: upper & lower extremity. *Acupuncture in Medicine*, 21(4), 112–122.

Pfuhl, W. (1934) Das subakromiale Nebengelenk des Schultergelenks. *Gegenbaurs Morphologisches Jahrbuch*, 73, 300–346.

Pusztaszeri, M.P., Seelentag, W. & Bosman, F.T. (2006) Immunohistochemical expression of endothelial markers CD31, CD34, von Willebrand factor, and Fli-1 in normal human tissues. *Journal of Histochemistry & Cytochemistry*, 54(4), 385–395.

Radas, C.B. & Pieper, H.-G. (2004) The coracoid impingement of the subscapularis tendon: a cadaver study. *Journal of Shoulder and Elbow Surgery*, 13(2), 154–159.

Rathbun, J.B. & Macnab, I. (1970) The microvascular pattern of the rotator cuff. *Journal of Bone & Joint Surgery*, 52-B(3), 540–553.

Rein, S., Hanisch, U., Zwipp, H., Fieguth, A., Lwowski, S. & Hagert, E. (2013) Comparative analysis of inter- and intraligamentous distribution of sensory nerve endings in ankle ligaments: a cadaver study. *Foot & Ankle International*, 34(7), 1017–1024.

Rockwood Jr., C.A., Matsen III, F.A., Wirth, M.A. & Lippitt, S.B. (2009) *The shoulder*, 4th edition. Saunders Elsevier.

Ross, M.H. (2006) *Histology: a text and atlas with correlated cell and molecular biology*, 5th edition. Lippincott Wiliams & Wilkins.

Rosse, C. & Gaddum-Rosse, P. (1997) *Hollinshead's textbook of anatomy*, 5th edition. Lippincott-Raven.

Sarkar, K. & Uhthoff, H. (1983) Ultrastructure of the subacromial bursa in painful shoulder syndromes. *Virchows Archiv A, Pathological Anatomy and Histopathology*, 400(2), 107–117.

Schraner, A.B. & Major, N.M. (1999) MR imaging of the subcoracoid bursa. *American Journal of Roentgenology*, 172(6), 1567–1571.

Seitz, A.L. & Michener, A. (2011) Ultrasonographic measures of subacromial space in patients with rotator cuff disease: a systematic review. *Journal of Clinical Ultrasound*, 39(3), 146–154.

Seo, C.M., Kim, K., Jeon, A., Uhm, C.S., Lee, J.H. & Han, S.H. (2018) Clinical anatomy for the innervated pattern and boundary of the subdeltoid bursa. *BioMed Research International*, 2018, 4535031.

Smith, M.D. (2011) The normal synovium. *The Open Rheumatology Journal*, 5, 100–106.

Soifer, T.B., Levy, H.J., Miller Soifer, F., Kleinbart, F., Vigorita, V. & Bryk, E. (1996) Neurohistology of the subacromial space. *Arthroscopy*, 12(2), 182–186.

Standring, S. (2016) *Gray's anatomy: the anatomical basis of clinical practice*, 41st edition. Elsevier.

Stecco, C., Macchi, V., Barbieri, A., Tiengo, C., Porzionato, A. & De Caro, R. (2018) Hand fasciae innervation: the palmar aponeurosis. *Clinical Anatomy*, 31(5), 677–683.

Steinbeck, J., Liljenqvist, U. & Jerosch, J. (1998) The anatomy of the glenohumeral ligamentous complex and its contribution to anterior shoulder stability. *Journal of Shoulder and Elbow Surgery*, 7(2), 122–126.

Strizak, A.M., Danzig, L., Jackson, D.W., Resnick, D. & Staple, T. (1982) Subacromial bursography. An anatomical and clinical study. *Journal of Bone & Joint Surgery - American*, 64(2), 196–201.

Suvarna, S.K., Layton, C. & Bancroft, J.D. (2013) *Bancroft's theory and practice of histological techniques*, 7th edition. Churchill Livingstone.

Tallia, A.F. & Cardone, D.A. (2003) Diagnostic and therapeutic injection of the shoulder region. *American Family Physician*, 67(6), 1271–1278.

Taylor, W. (2005) Musculoskeletal pain in the adult New Zealand population: prevalence and impact. *The New Zealand Medical Journal*, 118(1221), 22–36.

Tomita, Y., Ozaki, J., Sakurai, G., Kondo, T., Nakagaki, K. & Tamai, S. (1997) Neurohistology of the subacromial bursa in rotator cuff tear. *Journal of Orthopaedic Science*, 2(5), 295–300.

Uhthoff, H.K. & Sarkar, K. (1991) Surgical repair of rotator cuff ruptures. The importance of the subacromial bursa. *Journal of Bone & Joint Surgery*, 73-B(3), 399–401.

Vangsness Jr., C.T., Ennis, M., Taylor, J.G. & Atkinson, R. (1995) Neural anatomy of the glenohumeral ligaments, labrum, and subacromial bursa. *Arthroscopy*, 11(2), 180–184.

Verdú, E., Ceballos, D., Vilches, J.J. & Navarro, X. (2000) Influence of aging on peripheral nerve function and regeneration. *Journal of the Peripheral Nervous System*, 5(4), 191–208.

Whittaker, C.R. (1910) The arrangement of the bursae in the superior extremities of the full-time foetus. *Journal of Anatomy and Physiology*, 44(2), 133–136.

Wilkinson, L.S. & Edwards, J.C.W. (1989) Microvascular distribution in normal human synovium. *Journal of Anatomy*, 167, 129–136.

Witherspoon, J.W., Smirnova, I.V. & McIff, T. (2014) Improved gold chloride staining method for anatomical analysis of sensory nerve endings in the shoulder capsule and labrum as examples of loose and dense fibrous tissues. *Biotechnic & Histochemistry*, 89(5), 355–370.

Woodley, S.J., Mercer, S.R. & Nicholson, H.D. (2008) Morphology of the bursae associated with the greater trochanter of the femur. *The Journal of Bone and Joint Surgery. American*, 90(2), 284–294.

Yang, H.-F., Tang, K.-L., Chen, W., Dong, S.-W., Jin, T., Gong, J.-C. et al. (2009) An anatomic and histologic study of the coracohumeral ligament. *Journal of Shoulder and Elbow Surgery*, 18(2), 305–310.

Yeo, E.D., Rhyu, I.J., Kim, H.J., Kim, D.S., Ahn, J.-H. & Lee, Y.K. (2016) Can Bassett's ligament be removed? *Knee Surgery, Sports Traumatology, Arthroscopy*, 24(4), 1236–1242.

Yepes, H., Al-Hibshi, A., Tang, M., Morris, S.F. & Stanish, W.D. (2007) Vascular anatomy of the subacromial space: a map of bleeding points for the arthroscopic surgeon. *Arthroscopy*, 23(9), 978–984.

Zimny, M.L. (1988) Mechanoreceptors in articular tissues. *American Journal of Anatomy*, 182(1), 16–32.

SUPPORTING INFORMATION

Additional supporting information may be found in the online version of the article at the publisher's website.

How to cite this article: Kennedy, M.S., Nicholson, H.D. & Woodley, S.J. (2022) The morphology of the subacromial and related shoulder bursae. An anatomical and histological study. *Journal of Anatomy*, 240, 941–958. Available from: https://doi.org/10.1111/joa.13603